

## Evaluation of the Effect of Different Mesenchymal Stem Cell Microvesicles on Diabetic Wound Healing

 Cemal Alper Kemalolu,<sup>1</sup>  Ömer Taşkın,<sup>2</sup>  Zeynep Burçin Gönen,<sup>3</sup>  
 Arzu Hanım Yay,<sup>4</sup>  Ferhat Bozkurt<sup>5</sup>

<sup>1</sup>Department of Plastic, Reconstructive and Aesthetic Surgery, Memorial Ankara Hospital, Ankara, Türkiye

<sup>2</sup>Department of Plastic, Reconstructive and Aesthetic Surgery, Malatya Training and Research Hospital, Malatya, Türkiye

<sup>3</sup>Department of Oral and Maxillofacial Surgery, Genome and Stem Cell Centre, Erciyes University, Kayseri, Türkiye

<sup>4</sup>Department of Histology and Embryology, Erciyes University, Kayseri, Türkiye

<sup>5</sup>Department of Plastic, Reconstructive and Aesthetic Surgery, Erciyes University, Kayseri, Türkiye



### Cite this article as:

Kemaloğlu CA, Taşkın Ö, Gönen ZB, Hanım Yay A, Bozkurt F. Evaluation of the Effect of Different Mesenchymal Stem Cell Microvesicles on Diabetic Wound Healing. J Clin Pract Res 2026;48(0):0–0.

### Address for correspondence:

Ferhat Bozkurt.  
Department of Plastic, Reconstructive and Aesthetic Surgery, Erciyes University, Kayseri, Türkiye  
**Phone:** +90 352 207 66 66  
**E-mail:** ferhatbozkurt@erciyes.edu.tr

**Submitted:** 13.10.2025

**Revised:** 10.02.2026

**Accepted:** 11.02.2026

**Available Online:** 27.02.2026

Erciyes University Faculty of Medicine Publications - Available online at [www.jcprres.com](http://www.jcprres.com)

### ABSTRACT

**Objective:** Mesenchymal stem cell (MSC)-derived microvesicles play a pivotal role in the regenerative cascade of wound healing. This study aimed to comparatively evaluate the therapeutic potential of microvesicles isolated from different MSC sources in the healing of diabetic cutaneous wounds.

**Materials and Methods:** Forty Wistar albino rats were randomly assigned to four experimental groups (n=10 per group). Following the induction of diabetes and the creation of full-thickness circular dorsal skin defects, each group received a distinct treatment: Group 1 received saline (control), Group 2 received adipose-derived stem cell microvesicles (ADSC-MVs), Group 3 received umbilical cord-derived stem cell microvesicles (UCDSC-MVs), and Group 4 received bone marrow-derived stem cell microvesicles (BMDSC-MVs). Outcomes related to re-epithelialization, neovascularization, and collagen matrix formation were evaluated both macroscopically and histologically.

**Results:** The microvesicle-treated groups demonstrated faster wound closure and improved collagen fiber alignment compared with the control group. Angiogenic activity was increased in all treatment groups, with the most pronounced effects observed in the UCDSC-MVs group. Notably, the UCDSC-MVs group exhibited a significantly greater epithelial tongue length than the control group on postoperative days 3 and 14 (p=0.008 and p<0.001, respectively).

**Conclusion:** These findings indicate that UCDSC-MVs possess a superior capacity to promote re-epithelialization and may represent an effective cell-free therapeutic approach for diabetic wound repair.

**Keywords:** Diabetes wound, mesenchymal stem cells, microvesicles, regeneration, wound healing.



## INTRODUCTION

A wound represents a discontinuity or disruption in the integrity of living tissue. Effective repair of such injuries is essential to maintain tissue function and prevent systemic infection. The wound-healing process progresses through several overlapping yet coordinated phases: hemostasis, inflammation, proliferation, and remodeling.<sup>1</sup> These phases may be impaired by various systemic conditions, notably diabetes mellitus (DM), hypertension, obesity, and certain rheumatologic or inflammatory disorders.<sup>2–4</sup>

Diabetes mellitus is a chronic metabolic disorder that significantly delays the wound-healing cascade due to persistent hyperglycemia, microvascular dysfunction, peripheral neuropathy, and chronic inflammation.<sup>5,6</sup> It is estimated that 15–25% of individuals with diabetes will develop diabetic foot ulcers (DFUs) during their lifetime.<sup>7</sup> Despite advances in medical care, the clinical management of DFUs is largely dependent on conservative approaches, and a fully effective treatment strategy has yet to be established. Therefore, the development of new therapeutic strategies aimed at accelerating diabetic wound repair remains an urgent clinical priority.

Mesenchymal stem cells (MSCs) have emerged as a potential regenerative therapy for impaired wound healing, primarily through their paracrine secretion of bioactive molecules, including cytokines and growth factors.<sup>8–11</sup> These multipotent, fibroblast-like, non-hematopoietic cells can be harvested from multiple sources, including bone marrow, adipose tissue, and umbilical cord. Increasing evidence suggests that the therapeutic activity of MSCs is largely mediated by small extracellular vesicles known as microvesicles (MSC-MVs), rather than by direct cell replacement.

Microvesicles are membrane-bound nanoparticles measuring 100–1000 nm and carry diverse cargo, including proteins, lipids, DNA, and regulatory RNAs.<sup>12</sup> Numerous investigations have confirmed that MSC-derived microvesicles from different tissue origins contribute to wound repair through distinct molecular constituents and signaling effects.<sup>13</sup> Nevertheless, comparative *in vivo* evaluations of microvesicles derived from various MSC sources in the context of wound healing remain limited. The present study was therefore designed to assess and compare the wound-healing efficacy of microvesicles isolated from adipose-derived stem cells (ADSC), umbilical-cord-derived stem cells (UCDSC), and bone-marrow-derived stem cells (BMDSC) in a diabetic rat model. Determining which MSC-microvesicle source yields the strongest regenerative response may help refine future cell-free therapeutic strategies for DFU management.

## KEY MESSAGES

- Mesenchymal stem cells provide new therapeutic tools in the management of diabetic wounds; however, challenges related to storage, potential immune rejection, and ethical concerns continue to limit their clinical use.
- Mesenchymal stem cell-derived microvesicles offer similar biologic advantages in wound healing without the drawbacks associated with stem cell-based therapies.
- Umbilical cord-derived stem cell microvesicles demonstrate a superior capacity for re-epithelization, which may play an important role in cell-free diabetic wound management.

## MATERIALS AND METHODS

### Microvesicle Isolation and Characterization

Mesenchymal stem cells were supplied by the Good Manufacturing Practice (GMP) laboratory of the Erciyes University Genome and Stem Cell Center. Human ADSCs and BMDSCs were cultured in Dulbecco's Modified Eagle Medium (low glucose; Biological Industries, USA), whereas UCDSCs were maintained in Alpha Minimum Essential Medium ( $\alpha$ -MEM) supplemented with 10% serum, 1% antibiotics, and 1% stable L-glutamine (Biological Industries, USA), as previously described.<sup>14,15</sup>

The immunophenotypic profiles of MSCs were confirmed by flow cytometry (Beckman Coulter, USA) using antibodies against CD44, CD90, CD105, CD11b, CD19, and CD34 (BD Stem Flow hMSC Kit, USA).

When thawed MSCs reached approximately 90% confluence, the culture medium was replaced with serum-free medium, and the cells were incubated for an additional 24 hours to obtain conditioned medium (secretome). The collected secretomes were subjected to microvesicle isolation using a commercial precipitation-based isolation kit (ExoQuick-TC, System Biosciences, USA) in accordance with the manufacturer's instructions.<sup>16</sup> Briefly, the secretomes were centrifuged at 3000  $\times$  g for 15 minutes to remove cellular debris, and the resulting supernatants were mixed with the precipitation reagent at a 1:5 ratio. Following overnight incubation at 4°C, the mixtures were centrifuged at 1500  $\times$  g for 5 minutes to pellet the microvesicles.

The morphological features and size characteristics of the isolated microvesicles were evaluated using a scanning electron microscope (SEM) (Zeiss GEMINI 500, Germany). Size distribution and particle concentration were analyzed by nanoparticle

tracking analysis (NTA) using a NanoSight NS300 system (Malvern, UK), according to the manufacturer's protocol. Total protein concentration was determined by the Bradford assay (Bio-Rad, USA). Based on previous reports,<sup>17</sup> microvesicles were prepared at a final concentration of 200 µg/mL for administration to experimental animals using a concentrator device (Eppendorf Concentrator Plus, Thermo Fisher Scientific, UK).

The term “microvesicle” is used throughout the manuscript to describe extracellular vesicles isolated by a precipitation-based method. Given the isolation technique employed, the obtained vesicles likely represent a heterogeneous population of extracellular vesicles rather than a single vesicle subtype defined by biogenesis.

### Animals, Experimental Design, and Surgical Procedure

All animal experiments were conducted following approval from the Erciyes University Animal Experiments Ethics Committee (approval number: 22/265, date: 07.12.2022), and in accordance with international guidelines for the care and use of laboratory animals.

A priori power analysis was performed to determine the appropriate sample size, based on previously reported differences in wound closure outcomes in diabetic wound models. Accordingly, 40 male Wistar albino rats (weighing 213–330 g) were included in the study. DM was induced by intraperitoneal injection of streptozotocin (55 mg/kg; Sigma-Aldrich, USA). Blood glucose levels were measured from tail vein samples 48 hours after injection, and animals with glucose levels  $\geq 250$  mg/dL were considered diabetic.

The rats were randomly allocated into four experimental groups (n=10 per group):

- Group 1: Saline (control)
- Group 2: Bone-marrow-derived stem cell microvesicles (BMDSC-MVs)
- Group 3: Umbilical-cord-derived stem cell microvesicles (UCDSC-MVs)
- Group 4: Adipose-derived stem cell microvesicles (ADSC-MVs).

General anesthesia was achieved via intraperitoneal administration of ketamine hydrochloride (80 mg/kg) and xylazine (10 mg/kg). The dorsal skin was shaved and disinfected with povidone–iodine solution. Two circular, full-thickness excisional wounds (2 cm in diameter and spaced 2 cm apart) were created on the dorsal surface of each rat under sterile conditions. The experimental protocol was terminated on postoperative day 14, after which all animals were euthanized for tissue harvesting (Fig. 1).

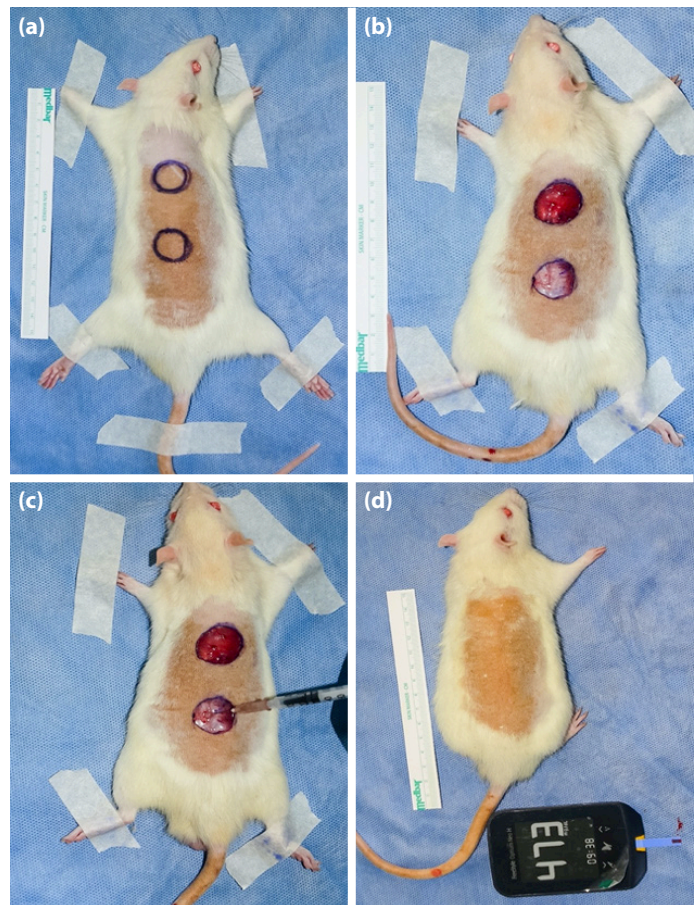


**Figure 1.** (a) Preparation of the surgical area and marking of full-thickness wounds. (b) Creation of wounds. (c) Injection of microvesicles into the wound sites. (d) Measurement of glucose levels from tail vein samples.

### Analysis of Wound Closure Rate

Digital images of the wounds were captured at a standardized distance of 50 cm using a Canon EOS 250D camera on postoperative days 0, 3, 5, 7, 10, and 14. Wound area measurements were performed using ImageJ software (NIH, USA) by an investigator blinded to the experimental groups.

To enable early histopathological evaluation, the cranial wound created in each animal was designated for biopsy sampling on postoperative day 3. As the biopsy procedure constitutes an additional surgical intervention that may influence the wound-healing process, the cranial wound was excluded from wound closure analysis. Accordingly, wound closure rates were assessed exclusively using the caudal wound, which was not subjected to any additional surgical manipulation. ImageJ-based wound area measurements were therefore performed solely on the caudal wound.

The wound closure rate was calculated using the following formula:

$$\text{Healing rate (\%)} = \frac{S_0 - S_A}{S_0} \times 100$$

where  $S_0$  represents the initial wound area on day 0, and  $S_A$  represents the wound area at the indicated postoperative time point.

### Histopathological Assessment

To avoid sampling-related interference between early and late healing phases, histopathological specimens were obtained from different wound sites at predefined time points. In each animal, the cranial wound was designated for early-stage histopathological evaluation, and a 3-mm full-thickness tissue specimen was harvested on postoperative day 3. For late-stage evaluation, a 3-mm full-thickness tissue specimen was obtained from the caudal wound on postoperative day 14.

Harvested tissues were fixed in 10% formalin for 24 hours, dehydrated through a graded ethanol series, cleared with xylene, and embedded in paraffin following incubation in a molten paraffin bath for two hours. Paraffin-embedded tissues were sectioned at a thickness of 5  $\mu\text{m}$  and stained with hematoxylin–eosin (H&E) and Masson's trichrome.

Light microscopic evaluation was performed using an Olympus BX-51 light microscope. Histological images were captured with a digital microscope camera (Zeiss, Germany) and analyzed using ImageJ software (NIH, USA) by an investigator blinded to the experimental groups.

Microscopic evaluation was performed using a light microscope. Epithelial tongue length ( $\mu\text{m}$ ) was measured as an objective indicator of re-epithelialization and was quantified using ImageJ software (NIH, USA) on images captured with a digital microscope camera (Zeiss, Germany). In addition, wound healing was evaluated semi-quantitatively according to the scoring system described by Galeano et al.<sup>18</sup> Within this system, epidermal regeneration and angiogenesis (granulation tissue formation) were scored on a 4-point scale, with higher scores indicating more advanced wound healing. Collagen deposition was assessed semi-quantitatively on Masson's trichrome–stained sections using a 4-point scoring system.

### Statistical Analysis

Statistical analyses were performed using SPSS version 22.0 (SPSS Inc., Chicago, IL, USA). Descriptive statistics were presented as mean  $\pm$  standard deviation (SD) for normally distributed variables and as median (interquartile range) for non-normally distributed or ordinal variables. Normality of data distribution was assessed using the Shapiro–Wilk test.

Wound closure analysis was performed using a single wound per animal to avoid clustering bias. Repeated wound area measurements obtained on postoperative days 0, 3, 5, 7, 10, and 14 were analyzed using repeated-measures analysis of variance (ANOVA) to account for within-animal correlations and to evaluate the effects of group, time, and group  $\times$  time interaction. The assumption of sphericity was assessed using Mauchly's test, and when violated, the Greenhouse–Geisser correction was applied. Accordingly, corrected degrees of freedom are reported.

Epithelial tongue length, which did not show a normal distribution, and histopathological scoring parameters (epidermal regeneration, angiogenesis, and fibrosis), which were ordinal variables, were compared among groups using the Kruskal–Wallis test, followed by Dunn's post hoc test for multiple comparisons. A  $p$  value  $<0.05$  was considered statistically significant.

## RESULTS

All animals successfully met the predefined criteria for diabetes induction prior to wound creation and were included in the subsequent analyses.

Two rats in the ADSC-MVs group and one rat in the BMDSC-MVs group died due to anesthesia-related complications. Accordingly, data analysis included eight animals in the ADSC-MVs group, nine in the BMDSC-MVs group, and 10 animals in each of the remaining two groups.

### Characterization of MSCs and MSC-Derived Microvesicles

All MSC cultures retained the typical spindle-shaped, fibroblast-like morphology. Flow cytometric immunophenotyping confirmed their mesenchymal phenotype. ADSCs expressed CD90 (99.87%), CD44 (98.1%), and CD105 (99.55%), while hematopoietic markers CD11b, CD19, and CD34 were nearly absent (0.84%). Similarly, BMDSCs expressed CD90 (99.84%), CD44 (99.55%), and CD105 (99.05%), with minimal expression of CD11b, CD19, and CD34 (0.25%). UCDSCs showed high expression of CD90 (99.8%), CD44 (95.72%), and CD105 (99.37%), with low positivity for CD11b, CD19, and CD34 (1.41%).

Scanning electron microscopy and nanoparticle tracking analysis confirmed vesicular morphology and particle size consistent with microvesicles (Fig. 2).

### Wound-Healing Rate

Wound area measurements derived from serial macroscopic images were compared across postoperative time points using repeated-measures ANOVA. The analysis demonstrated a significant main effect of time ( $F(2.90,$

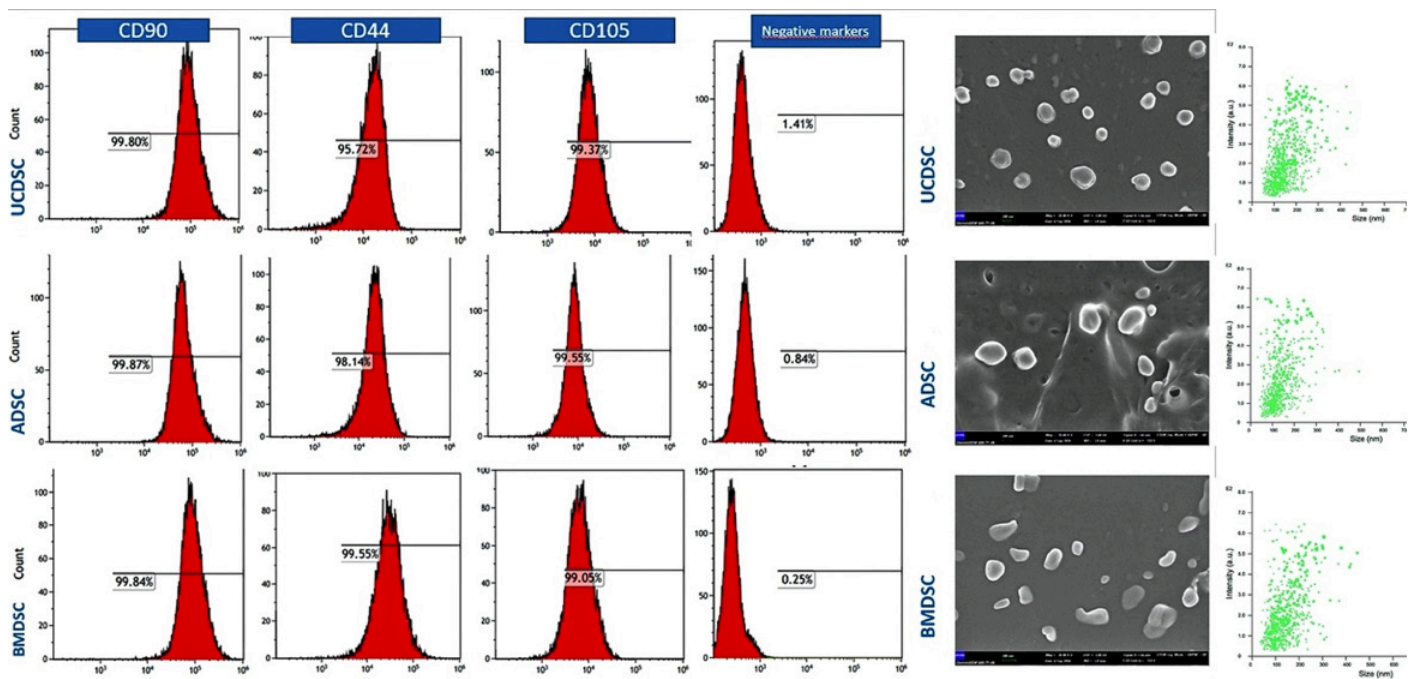


**Figure 2.** Flow cytometric analysis demonstrated that mesenchymal stem cells (MSCs) were positive for CD90, CD44, and CD105 and negative for CD11b, CD19, and CD34. Morphology of microvesicles was examined using scanning electron microscopy (SEM), and size distribution was analyzed by nanoparticle tracking analysis (NTA); scale bar=200 nm.

95.64)=278.98,  $p < 0.001$ ), a significant main effect of group ( $F(3, 33)=14.44$ ,  $p < 0.001$ ), and a significant time  $\times$  group interaction ( $F(8.70, 95.64)=6.72$ ,  $p < 0.001$ ). Overall, microvesicle-treated wounds exhibited significantly improved wound closure compared with saline-treated controls throughout the observation period. Bonferroni-adjusted post hoc analyses demonstrated that the control group exhibited significantly poorer wound-healing outcomes compared with the ADSC-MVs, UCDSC-MVs, and BMDSC-MVs groups (all  $p < 0.001$ ) (Table 1), whereas no statistically significant differences were observed among the microvesicle-treated groups ( $p > 0.05$ ). By postoperative day 14, wound closure outcomes were comparable among the three microvesicle-treated groups (Fig. 3, 4).

### Histological Findings

#### Epithelialization

Epithelial tongue length was evaluated on H&E-stained sections. On day 3, epithelial tongue length differed significantly among groups ( $p < 0.001$ ). Post hoc analysis demonstrated that the UCDSC-MVs group exhibited significantly greater epithelial tongue length compared with the control group ( $p = 0.008$ ) and the BMDSC-MVs group ( $p = 0.007$ ). No statistically significant differences were observed among the other microvesicle-treated groups.

**Table 1.** Results of repeated-measures analysis of variance (ANOVA) for wound closure rate

Effect	df	F	p
Time	2.90, 95.64	278.98	<0.001
Group	3, 33	14.44	<0.001
Time $\times$ group	8.70, 95.64	6.72	<0.001

Greenhouse–Geisser correction was applied when the assumption of sphericity was violated.

On day 14, epithelial tongue length also differed significantly among groups ( $p < 0.001$ ). The UCDSC-MVs group showed significantly greater epithelial tongue length compared with the control group ( $p < 0.001$ ), whereas no significant differences were detected among the microvesicle-treated groups (Table 2).

#### Angiogenesis

Angiogenic activity was assessed using Masson’s trichrome staining. On day 3, angiogenesis scores differed significantly among groups ( $p < 0.001$ ). Post hoc analysis revealed significantly higher angiogenesis scores in the UCDSC-MVs group compared with the control group ( $p < 0.001$ ) and the BMDSC-MVs group ( $p = 0.002$ ). No statistically significant difference was observed between the control and ADSC-MVs groups.

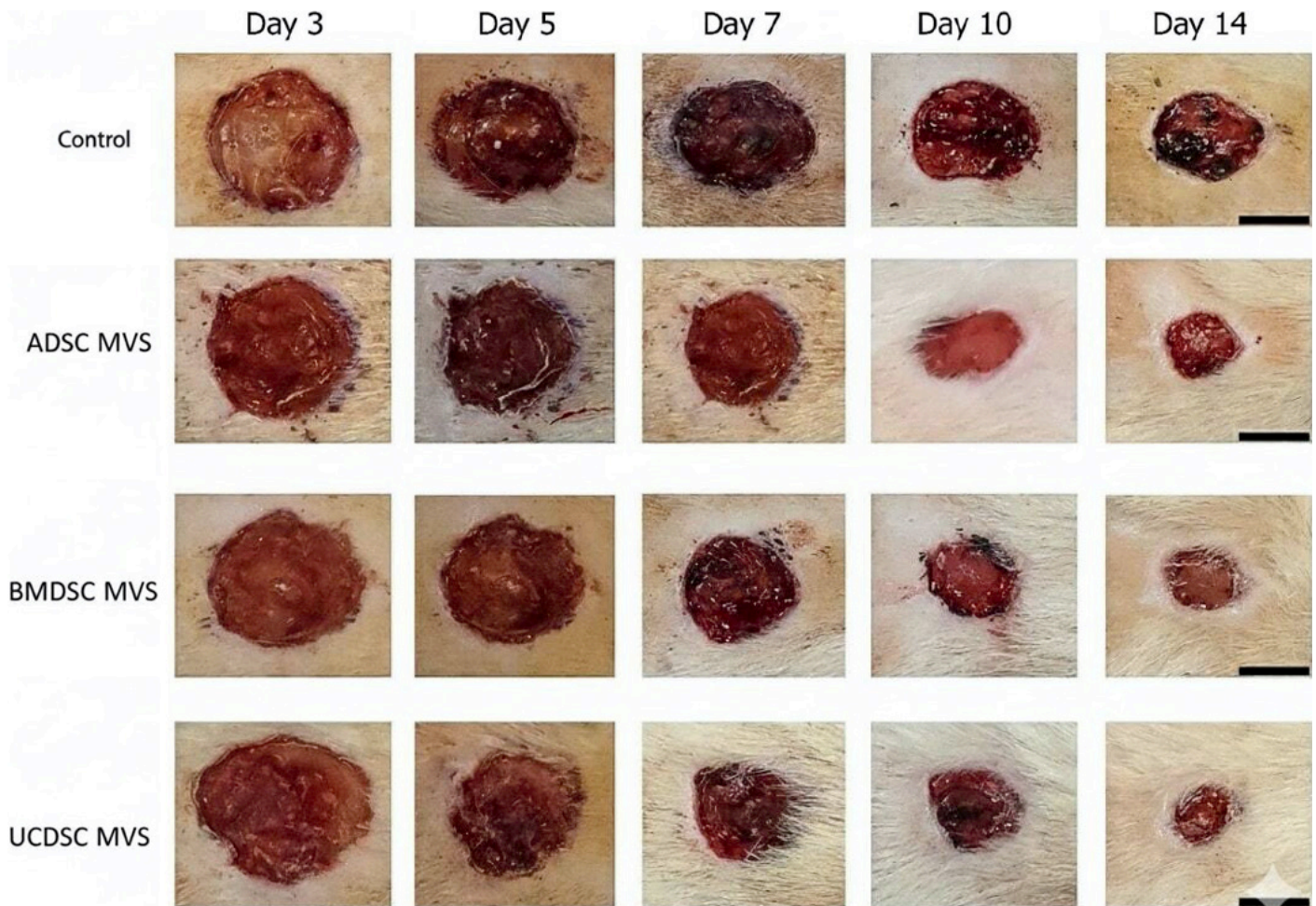


**Figure 3.** Images of the wound-healing process in all groups; scale bar=1 cm.

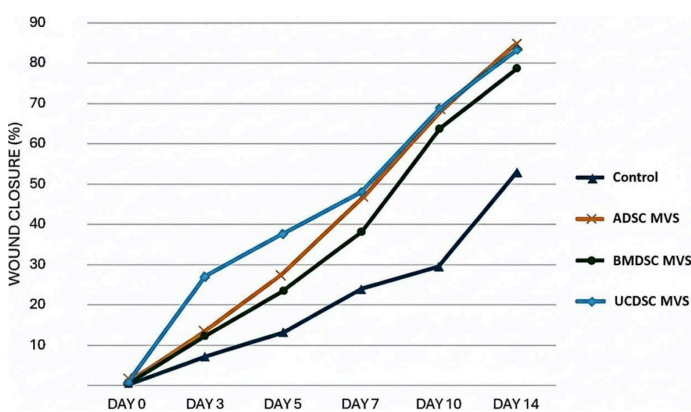


**Figure 4.** Wound closure rates among all groups.

On day 14, angiogenesis scores remained significantly different among groups ( $p=0.001$ ). Angiogenesis scores in the UCDC-MVs group were significantly higher than those in the

control group ( $p=0.039$ ), while no other intergroup differences reached statistical significance

#### **Collagen Deposition (Fibrosis)**

Fibrosis was evaluated using Masson's trichrome staining. On day 3, fibrosis scores differed significantly among groups ( $p<0.001$ ). Post hoc analysis showed significantly lower fibrosis scores in the UCDC-MVs and BMDSC-MVs groups compared with the control group (both  $p=0.001$ ). No significant differences were observed among the microvesicle-treated groups ( $p>0.05$ ).

On day 14, fibrosis scores also differed significantly among groups ( $p<0.001$ ). Fibrosis scores were significantly lower in the UCDC-MVs and BMDSC-MVs groups compared with the control group ( $p\leq 0.007$ ), whereas no statistically significant differences were detected among the microvesicle-treated groups (Fig. 5).

**Table 2.** Histological outcomes on postoperative day 3 and day 14

Parameter	Group	Day 3		Day 14	
		n	Median (25 <sup>th</sup> –75 <sup>th</sup> )	n	Median (25 <sup>th</sup> –75 <sup>th</sup> )
Epithelial tongue length (µm)	Control	10	<b>462.378 (400.104–560.538)</b>	10	<b>782.594 (694.162–871.263)</b>
	BMDSC-MVs	10	<b>512.738 (476.316–535.692)</b>	9	<b>906.574 (825.473–996.450)</b>
	UCDSC-MVs	10	<b>605.465 (524.705–765.569)*</b>	10	<b>1085.951 (1015.302–1346.942)*</b>
	ADSC-MVs	10	<b>498.831 (445.909–552.816)</b>	8	<b>828.584 (746.562–932.561)</b>
Angiogenesis score	Control	10	<b>1.0 (1.0–2.0)</b>	10	<b>2.0 (2.0–3.0)</b>
	BMDSC-MVs	10	<b>2.0 (2.0–2.0)</b>	9	<b>3.0 (3.0–3.0)</b>
	UCDSC-MVs	10	<b>3.0 (3.0–3.0)*</b>	10	<b>3.5 (3.0–4.0)*</b>
	ADSC-MVs	10	<b>2.0 (2.0–2.0)</b>	8	<b>2.5 (2.0–3.25)</b>
Fibrosis score	Control	10	<b>0.0 (0.0–1.0)</b>	10	<b>2.0 (2.0–2.0)</b>
	BMDSC-MVs	10	<b>0.0 (0.0–1.0)*</b>	9	<b>2.0 (2.0–2.0)*</b>
	UCDSC-MVs	10	<b>1.0 (1.0–1.0)*</b>	10	<b>2.0 (2.0–3.0)</b>
	ADSC-MVs	10	<b>0.0 (0.0–1.0)</b>	8	<b>2.0 (2.0–3.0)</b>
Epithelial regeneration score	Control	10	<b>1.0 (1.0–1.0)</b>	10	<b>1.0 (1.0–2.0)</b>
	BMDSC-MVs	10	<b>1.0 (1.0–2.0)</b>	9	<b>2.0 (1.0–2.0)</b>
	UCDSC-MVs	10	<b>2.0 (1.0–2.0)</b>	10	<b>2.0 (2.0–2.75)*</b>
	ADSC-MVs	10	<b>1.0 (1.0–1.0)</b>	8	<b>1.0 (1.0–2.0)</b>

Data are presented as median (25<sup>th</sup>–75<sup>th</sup> percentiles). Group comparisons were performed using the Kruskal–Wallis test followed by Dunn’s post hoc test. An asterisk (\*) indicates a statistically significant post hoc difference (p<0.05). Specific between-group comparisons are detailed in the Results section.

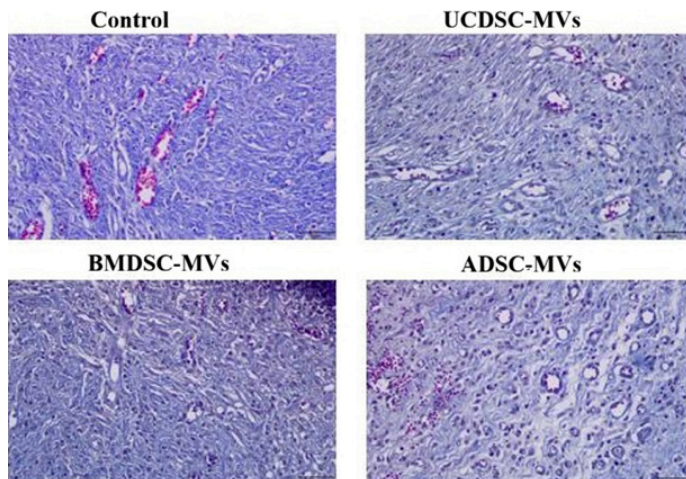


**Figure 5.** Masson’s trichrome–stained sections obtained from the control, umbilical cord–derived stem cell microvesicles (UCDSC-MVs), bone marrow–derived stem cell microvesicles (BMDSC-MVs), and adipose–derived stem cell microvesicles (ADSC-MVs) groups on postoperative day 14 (40× magnification; scale bar=50 µm). Well-organized collagen bundles are observed in the microvesicle-treated groups, whereas the control group shows a more disorganized collagen structure.

## DISCUSSION

Diabetes mellitus remains a major contributor to impaired wound healing, largely because of glucose-induced cellular toxicity. The primary mechanisms underlying this delay include microvascular dysfunction, peripheral neuropathy, and sustained inflammation.<sup>19</sup> Although surgical closure is often required for diabetic wounds, it cannot fully address the underlying vascular and neural injury that drives ulcer formation.

Emerging evidence suggests that transplantation of MSCs can enhance angiogenesis, modulate extracellular matrix (ECM) remodeling, and support keratinocyte function in DFUs.<sup>20–22</sup> MSCs contribute to tissue repair both by differentiating into endothelial or stromal cells and by secreting paracrine mediators that regulate immunity, suppress inflammation, and stimulate regeneration. Despite their therapeutic promise, MSC-based cell therapies face challenges such as storage instability, mutation-related tumorigenicity, immune rejection, and ethical limitations.<sup>23</sup> MSC-MVs offer a viable alternative, recapitulating many of the parent cells’ regenerative effects while avoiding these drawbacks.

Mesenchymal stem cell–derived microvesicles act as natural nanocarriers for the paracrine signaling factors of stem cells, thus representing a novel, cell-free therapeutic strategy for

wound repair. Their bioactive cargo, including cytokines such as vascular endothelial growth factor (VEGF), transforming growth factor beta 1 (TGF- $\beta$ 1), interleukin 6 (IL-6), and IL-10, as well as proteins, DNA, and noncoding RNAs, can be internalized by recipient cells, where it modulates the local microenvironment. Previous research has demonstrated that microvesicles obtained from various MSC sources can promote tissue regeneration, with ADSC-MVs, BMDSC-MVs, and UCDS-C-MVs being the most extensively studied.

Adipose-derived stem cell microvesicles have attracted particular attention due to their ease of isolation and abundant availability. These vesicles can promote endothelial progenitor cell proliferation, stimulate angiogenesis, optimize fibroblast function, and reduce ulcer size.<sup>24–26</sup> They also mitigate oxidative stress by reducing reactive oxygen species (ROS) generation and improving mitochondrial activity under hyperglycemic conditions.<sup>27</sup> BMDSC-MVs, another promising cell-free approach, have demonstrated similar benefits. Yu et al.<sup>28</sup> showed that atorvastatin-pretreated BMDSC-MVs enhanced angiogenesis and wound closure in diabetic rats, while Hu et al.<sup>29</sup> reported that pioglitazone pretreatment improved collagen organization, ECM remodeling, and vascularization. In comparison, UCDS-Cs are advantageous because of their low immunogenicity, rapid expansion, and ethical acceptability. UCDS-C-MVs have been shown to alleviate oxidative stress, promote fibroblast proliferation and migration, and augment the angiogenic activity of endothelial cells.<sup>30–33</sup> Despite these promising findings, no prior *in vivo* study has directly compared the wound-healing potential of microvesicles derived from different MSC sources within a diabetic model.

In the present study, all microvesicle-treated groups exhibited faster wound closure than controls. Although overall healing rates did not differ significantly among the microvesicle types, variations were observed at specific stages. Notably, epithelial tongue length was significantly greater in the UCDS-C-MVs group on days 3 and 14. Hoang et al.<sup>34</sup> similarly reported that only UCDS-C-MVs secreted high levels of TGF- $\beta$ , a potent regulator of keratinocyte migration. Moreover, UCDS-C-MVs are known to be enriched in miR-21-3p, which enhances re-epithelialization.<sup>35</sup>

Regarding angiogenesis, microvesicle treatment was associated with increased angiogenic activity compared with controls, with the most pronounced effects observed in the UCDS-C-MVs group. Although microvessel density varied among treatment groups, significant differences were primarily detected between the UCDS-C-MVs and control groups, particularly at earlier stages. Previous studies have shown that ADSC-, BMDSC-, and UCDS-C-derived vesicles can promote angiogenesis through distinct signaling pathways.<sup>36</sup>

For instance, UCDS-C-MVs act through Wnt/ $\beta$ -catenin signaling,<sup>31</sup> BMDSC-MVs via the TGF- $\beta$ /Smad axis,<sup>37</sup> and ADSC-MVs through modulation of the Delta-like 4 pathway.<sup>24</sup> These findings suggest that, while the molecular mediators may differ, microvesicle-based therapies can support angiogenic processes during wound healing.

Extracellular matrix remodeling, particularly collagen synthesis and degradation, is a pivotal determinant of scar quality. Although collagen scores did not differ significantly among the microvesicle-treated groups, treated wounds displayed more organized collagen bundles compared with controls. ADSC-MVs enhance fibroblast function by upregulating genes such as N-cadherin, cyclin-1, and proliferating cell nuclear antigen (PCNA),<sup>37–39</sup> whereas BMDSC-MVs exert antifibrotic effects by suppressing TGF- $\beta$ /Smad signaling and increasing TGF- $\beta$ 3 expression.<sup>37</sup> UCDS-C-MVs have also been shown to regulate fibroblast activity through inhibition of phosphatase and tensin homolog (PTEN), sprouty homolog 1 (SPRY1), and the TGF- $\beta$ 2/SMAD2 pathway.<sup>35,40</sup> Collectively, these findings support a beneficial role of microvesicle-based therapies in fibroblast-mediated tissue remodeling.

To the best of our knowledge, this work represents the first *in vivo* comparative evaluation of MSC-MVs from different sources for diabetic wound repair. While each microvesicle type offered unique advantages at particular stages of healing, several limitations merit consideration. First, although macroscopic and histological improvements were evident, the molecular mechanisms underlying these effects were not explored. Given that MSC-MVs carry a wide array of bioactive molecules that act synergistically on multiple cell types, single-pathway analyses may not fully explain their complex biological activity. Thus, more comprehensive molecular studies are required.

Second, despite providing a useful experimental model, rodent wounds differ from chronic human diabetic foot ulcers; therefore, our results may not directly translate to clinical outcomes. In addition, the ideal dose and frequency of MSC-MV administration remain undetermined. In this study, a single standardized local application was employed; however, varying doses or repeated treatments might yield different results. Further basic and translational research, followed by controlled clinical trials, is needed to establish optimal protocols and ensure the safe application of MSC-MVs in diabetic wound therapy.

Finally, although termed microvesicles, the vesicle population analyzed in this study may include other extracellular vesicle subtypes due to the precipitation-based isolation method; therefore, future studies incorporating molecular marker analysis are warranted for more precise subclassification.

## CONCLUSION

In conclusion, this study represents the first in vivo comparison of MSC-MVs from different tissue origins in the treatment of diabetic wounds. Our findings demonstrate that microvesicles obtained from adipose tissue, bone marrow, and umbilical cord stem cells accelerated wound closure following subcutaneous administration to diabetic skin defects. Angiogenic activity was enhanced, with the most pronounced effects observed in the UCDCS-MVs group. Among the tested microvesicles, umbilical cord-derived microvesicles exhibited a notably stronger ability to promote re-epithelialization, highlighting their potential as a promising, cell-free therapeutic option for diabetic wound management.

**Ethics Committee Approval:** Ethics committee approval was obtained from Erciyes University Animal Experiments Ethics Committee (date: 07.12.2022, number: 22/265).

**Informed Consent:** Informed consent was not required for this study.

**Conflict of Interest:** The authors have no conflicts of interest to declare.

**Financial Disclosure:** This work was supported by the Research Fund (TTU-2023-12956) of Erciyes University.

**Use of AI for Writing Assistance:** No use of AI-assisted technologies was declared by the authors.

**Author Contributions:** Concept – CAK, ÖT, ZBG, AHY, FB; Design – CAK, ÖT, ZBG, AHY, FB; Supervision – CAK, ÖT, ZBG, AHY, FB; Resource – CAK, ÖT, ZBG, AHY; Materials – CAK, ÖT, ZBG, AHY; Data Collection and/or Processing – CAK, ÖT, ZBG, AHY; Analysis and/or Interpretation – CAK, ÖT, ZBG, AHY; Literature Review – CAK, ÖT, ZBG, AHY; Writing – CAK, ÖT, ZBG, AHY, FB; Critical Review – CAK, ÖT, ZBG, AHY, FB.

**Acknowledgments:** Authors are thankful to iconics (<https://iconics.com.tr>) for the graphics.

**Peer-review:** Externally peer-reviewed.

## REFERENCES

- Lindley LE, Stojadinovic O, Pastar I, Tomic-Canic M. Biology and Biomarkers for Wound Healing. *Plast Reconstr Surg* 2016;138(3 Suppl):185-285. [CrossRef]
- Goldman R. Growth factors and chronic wound healing: past, present, and future. *Adv Skin Wound Care* 2004;17(1):24-35. [CrossRef]
- Guo S, Dipietro LA. Factors affecting wound healing. *J Dent Res* 2010;89(3):219-29. [CrossRef]
- Falanga V. Wound healing and its impairment in the diabetic foot. *Lancet* 2005;366(9498):1736-43. [CrossRef]
- Holl J, Kowalewski C, Zimek Z, Fiedor P, Kaminski A, Oldak T, et al. Chronic Diabetic Wounds and Their Treatment with Skin Substitutes. *Cells* 2021;10(3):655. [CrossRef]
- Tsourdi E, Barthel A, Rietzsch H, Reichel A, Bornstein SR. Current aspects in the pathophysiology and treatment of chronic wounds in diabetes mellitus. *Biomed Res Int* 2013;2013:385641. [CrossRef]
- Boulton AJ, Vileikyte L, Ragnarson-Tennvall G, Apelqvist J. The global burden of diabetic foot disease. *Lancet* 2005;366(9498):1719-24. [CrossRef]
- Jeon YK, Jang YH, Yoo DR, Kim SN, Lee SK, Nam MJ. Mesenchymal stem cells' interaction with skin: wound-healing effect on fibroblast cells and skin tissue. *Wound Repair Regen* 2010;18(6):655-61. [CrossRef]
- Li H, Fu X. Mechanisms of action of mesenchymal stem cells in cutaneous wound repair and regeneration. *Cell Tissue Res* 2012;348(3):371-7. [CrossRef]
- Huayllani MT, Sarabia-Estrada R, Restrepo DJ, Boczar D, Sisti A, Nguyen JH, et al. Adipose-derived stem cells in wound healing of full-thickness skin defects: a review of the literature. *J Plast Surg Hand Surg* 2020;54(5):263-79. [CrossRef]
- Sorice S, Rustad KC, Li AY, Gurtner GC. The Role of Stem Cell Therapeutics in Wound Healing: Current Understanding and Future Directions. *Plast Reconstr Surg* 2016;138(3 Suppl):315-415. [CrossRef]
- Théry C, Zitvogel L, Amigorena S. Exosomes: composition, biogenesis and function. *Nat Rev Immunol* 2002;2(8):569-79. [CrossRef]
- Cabral J, Ryan AE, Griffin MD, Ritter T. Extracellular vesicles as modulators of wound healing. *Adv Drug Deliv Rev* 2018;129:394-406. [CrossRef]
- Uzun E, Güney A, Gönen ZB, Özkul Y, Kafadar İH, Günay M, et al. Intralesional allogeneic adipose-derived stem cells application in chronic diabetic foot ulcer: Phase I/2 safety study. *Foot Ankle Surg* 2021;27(6):636-42. [CrossRef]
- Oner A, Gonen ZB, Sevim DG, Sinim Kahraman N, Unlu M. Six-month results of suprachoroidal adipose tissue-derived mesenchymal stem cell implantation in patients with optic atrophy: a phase 1/2 study. *Int Ophthalmol* 2019;39(12):2913-22. [CrossRef]
- Bahar D, Gonen ZB, Gumusderelioglu M, Onger ME, Tokak EK, Ozturk-Kup F, et al. Repair of Rat Calvarial Bone Defect by Using Exosomes of Umbilical Cord-Derived Mesenchymal Stromal Cells Embedded in Chitosan/Hydroxyapatite Scaffolds. *Int J Oral Maxillofac Implants* 2022;37(5):943-50. [CrossRef]
- Kemaloğlu CA, Dursun EN, Yay AH, Gökdemir NS, Mat ÖC, Gönen ZB. The Optimal Effective Dose of Adipose-Derived Stem Cell Exosomes in Wound Healing. *Ann Plast Surg* 2024;93(2):253-60. [CrossRef]

18. Galeano M, Altavilla D, Cucinotta D, Russo GT, Calò M, Bitto A, et al. Recombinant human erythropoietin stimulates angiogenesis and wound healing in the genetically diabetic mouse. *Diabetes* 2004;53(9):2509-17. [\[CrossRef\]](#)
19. Liu Y, Liu Y, He W, Mu X, Wu X, Deng J, et al. Fibroblasts: Immunomodulatory factors in refractory diabetic wound healing. *Front Immunol* 2022;13:918223. [\[CrossRef\]](#)
20. Cao Y, Gang X, Sun C, Wang G. Mesenchymal Stem Cells Improve Healing of Diabetic Foot Ulcer. *J Diabetes Res* 2017;2017:9328347. [\[CrossRef\]](#)
21. Kato J, Kamiya H, Himeno T, Shibata T, Kondo M, Okawa T, et al. Mesenchymal stem cells ameliorate impaired wound healing through enhancing keratinocyte functions in diabetic foot ulcerations on the plantar skin of rats. *J Diabetes Complications* 2014;28(5):588-95. [\[CrossRef\]](#)
22. Shi R, Jin Y, Cao C, Han S, Shao X, Meng L, et al. Localization of human adipose-derived stem cells and their effect in repair of diabetic foot ulcers in rats. *Stem Cell Res Ther* 2016;7(1):155. [\[CrossRef\]](#)
23. Mazini L, Rochette L, Admou B, Amal S, Malka G. Hopes and Limits of Adipose-Derived Stem Cells (ADSCs) and Mesenchymal Stem Cells (MSCs) in Wound Healing. *Int J Mol Sci* 2020;21(4):1306. [\[CrossRef\]](#)
24. Liang X, Zhang L, Wang S, Han Q, Zhao RC. Exosomes secreted by mesenchymal stem cells promote endothelial cell angiogenesis by transferring miR-125a. *J Cell Sci* 2016;129(11):2182-9. [\[CrossRef\]](#)
25. Li X, Xie X, Lian W, Shi R, Han S, Zhang H, et al. Exosomes from adipose-derived stem cells overexpressing Nrf2 accelerate cutaneous wound healing by promoting vascularization in a diabetic foot ulcer rat model. *Exp Mol Med* 2018;50(4):1-14. [\[CrossRef\]](#)
26. Wang M, Wang C, Chen M, Xi Y, Cheng W, Mao C, et al. Efficient Angiogenesis-Based Diabetic Wound Healing/Skin Reconstruction through Bioactive Antibacterial Adhesive Ultraviolet Shielding Nanodressing with Exosome Release. *ACS Nano* 2019;13(9):10279-93. [\[CrossRef\]](#)
27. Zhang Y, Bai X, Shen K, Luo L, Zhao M, Xu C, et al. Exosomes Derived from Adipose Mesenchymal Stem Cells Promote Diabetic Chronic Wound Healing through SIRT3/SOD2. *Cells* 2022;11(16):2568. [\[CrossRef\]](#)
28. Yu M, Liu W, Li J, Lu J, Lu H, Jia W, et al. Exosomes derived from atorvastatin-pretreated MSC accelerate diabetic wound repair by enhancing angiogenesis via AKT/eNOS pathway. *Stem Cell Res Ther* 2020;11(1):350. [\[CrossRef\]](#)
29. Hu Y, Tao R, Chen L, Xiong Y, Xue H, Hu L, et al. Exosomes derived from pioglitazone-pretreated MSCs accelerate diabetic wound healing through enhancing angiogenesis. *J Nanobiotechnology* 2021;19(1):150. [\[CrossRef\]](#)
30. Yang J, Chen Z, Pan D, Li H, Shen J. Umbilical Cord-Derived Mesenchymal Stem Cell-Derived Exosomes Combined Pluronic F127 Hydrogel Promote Chronic Diabetic Wound Healing and Complete Skin Regeneration. *Int J Nanomedicine* 2020;15:5911-26. [\[CrossRef\]](#)
31. Zhang B, Wu X, Zhang X, Sun Y, Yan Y, Shi H, et al. Human umbilical cord mesenchymal stem cell exosomes enhance angiogenesis through the Wnt4/ $\beta$ -catenin pathway. *Stem Cells Transl Med* 2015;4(5):513-22. [\[CrossRef\]](#)
32. Liu J, Yan Z, Yang F, Huang Y, Yu Y, Zhou L, et al. Exosomes Derived from Human Umbilical Cord Mesenchymal Stem Cells Accelerate Cutaneous Wound Healing by Enhancing Angiogenesis through Delivering Angiopoietin-2. *Stem Cell Rev Rep* 2021;17(2):305-17. [\[CrossRef\]](#)
33. Teng L, Maqsood M, Zhu M, Zhou Y, Kang M, Zhou J, et al. Exosomes Derived from Human Umbilical Cord Mesenchymal Stem Cells Accelerate Diabetic Wound Healing via Promoting M2 Macrophage Polarization, Angiogenesis, and Collagen Deposition. *Int J Mol Sci* 2022;23(18):10421. [\[CrossRef\]](#)
34. Hoang DH, Nguyen TD, Nguyen HP, Nguyen XH, Do PTX, Dang VD, et al. Differential Wound Healing Capacity of Mesenchymal Stem Cell-Derived Exosomes Originated From Bone Marrow, Adipose Tissue and Umbilical Cord Under Serum- and Xeno-Free Condition. *Front Mol Biosci* 2020;7:119. [\[CrossRef\]](#)
35. Hu Y, Rao SS, Wang ZX, Cao J, Tan YJ, Luo J, et al. Exosomes from human umbilical cord blood accelerate cutaneous wound healing through miR-21-3p-mediated promotion of angiogenesis and fibroblast function. *Theranostics* 2018;8(1):169-84. [\[CrossRef\]](#)
36. Zhou C, Zhang B, Yang Y, Jiang Q, Li T, Gong J, et al. Stem cell-derived exosomes: emerging therapeutic opportunities for wound healing. *Stem Cell Res Ther* 2023;14(1):107. [\[CrossRef\]](#)
37. Jiang T, Wang Z, Sun J. Human bone marrow mesenchymal stem cell-derived exosomes stimulate cutaneous wound healing mediates through TGF- $\beta$ /Smad signaling pathway. *Stem Cell Res Ther* 2020;11(1):198. [\[CrossRef\]](#)
38. Wang L, Hu L, Zhou X, Xiong Z, Zhang C, Shehada HMA, et al. Exosomes secreted by human adipose mesenchymal stem cells promote scarless cutaneous repair by regulating extracellular matrix remodelling. *Sci Rep* 2017;7(1):13321. Erratum in: *Sci Rep* 2018;8(1):7066. Erratum in: *Sci Rep* 2021;11(1):3245. [\[CrossRef\]](#)
39. Hu L, Wang J, Zhou X, Xiong Z, Zhao J, Yu R, et al. Exosomes derived from human adipose mesenchymal stem cells accelerates cutaneous wound healing via optimizing the characteristics of fibroblasts. *Sci Rep* 2016;6:32993.

- Erratum in: Sci Rep 2020;10(1):6693. Erratum in: Sci Rep 2026;16(1):2649. [\[CrossRef\]](#)
40. Fang S, Xu C, Zhang Y, Xue C, Yang C, Bi H, et al. Umbilical Cord-Derived Mesenchymal Stem Cell-Derived Exosomal MicroRNAs Suppress Myofibroblast Differentiation by Inhibiting the Transforming Growth Factor- $\beta$ /SMAD2 Pathway During Wound Healing. Stem Cells Transl Med 2016;5(10):1425-39. [\[CrossRef\]](#)